2022

Cardiac Gene Therapy With Relaxin Receptor 1 Overexpression Protects Against Acute Myocardial Infarction

Teja Devarakonda
Virginia Commonwealth University, devarakondstv@vcu.edu

Adolfo G. Mauro
Virginia Commonwealth University, amauro@vcu.edu

Chad Cain
Virginia Commonwealth University

Anindita Das
Virginia Commonwealth University, adas2@vcu.edu

Fadi N. Salloum
Virginia Commonwealth University, fnsalloum@vcu.edu

JACC: BASIC TO TRANSLATIONAL SCIENCE VOL. 7, NO. 1, 2022

PRECLINICAL RESEARCH

Cardiac Gene Therapy With Relaxin Receptor 1 Overexpression Protects Against Acute Myocardial Infarction

Teja Devarakonda, BS,[a,b] Adolfo G. Mauro, PhD,[a] Chad Cain, BS,[a] Anindita Das, PhD,[a] Fadi N. Salloum, PhD[a,b]

VISUAL ABSTRACT

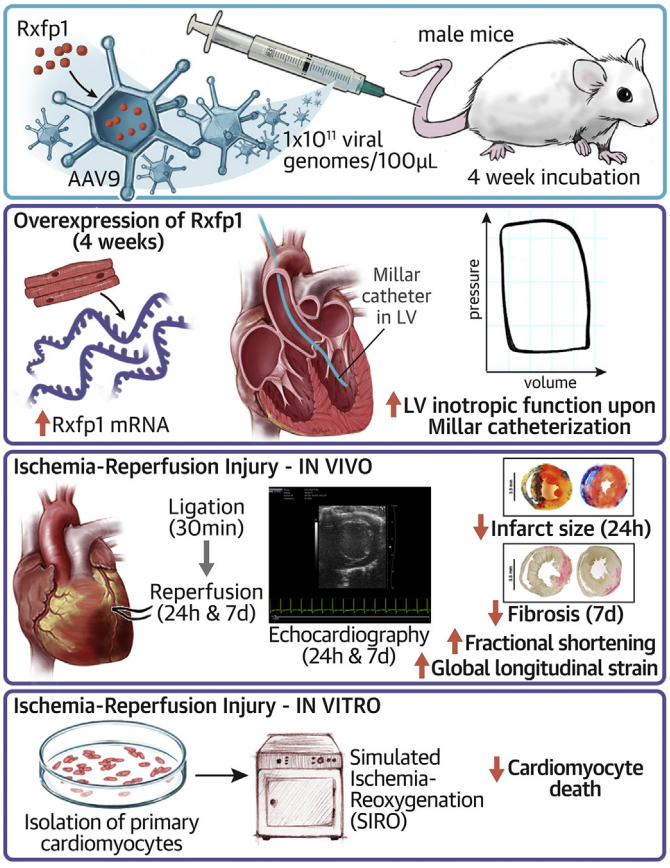

Devarakonda, T. et al. J Am Coll Cardiol Basic Trans Science. 2022;7(1):53-63.

HIGHLIGHTS

- **AAV9 vectors can upregulate Rxfp1 mRNA in murine heart after intravenous injection.**
- **RXFP1 upregulation sensitizes the left ventricle to relaxin-induced inotropy.**
- **RXFP1 overexpression protects heart from ischemia-reperfusion injury.**

From the [a]Pauley Heart Center, Division of Cardiology, Department of Internal Medicine, Virginia Commonwealth University, Richmond, Virginia, USA; and the [b]Department of Physiology and Biophysics, Virginia Commonwealth University, Richmond, Virginia, USA.

The authors attest they are in compliance with human studies committees and animal welfare regulations of the authors' institutions and Food and Drug Administration guidelines, including patient consent where appropriate. For more information, visit the Author Center.

Manuscript received July 26, 2021; revised manuscript received October 13, 2021, accepted October 16, 2021.

ISSN 2452-302X https://doi.org/10.1016/j.jacbts.2021.10.012

ABBREVIATIONS AND ACRONYMS

AAV = adeno-associated virus

CMV = cytomegalovirus

eNOS = endothelial nitric oxide synthase

GLS = global longitudinal strain

IR = ischemia-reperfusion

LV = left ventricular

MAPK = mitogen-activated protein kinase

MI = myocardial infarction

mRNA = messenger ribonucleic acid

PV = pressure-volume

RXFP1 = relaxin family peptide receptor 1

SIRO = simulated ischemia and reoxygenation

VEC = empty vector

SUMMARY

Relaxin is a pleiotropic hormone shown to confer cardioprotection in several preclinical models of cardiac ischemia-reperfusion injury. In the present study, the effects of up-regulating relaxin family peptide receptor 1 (RXFP1) via adeno-associated virus serotype 9 (AAV9) vectors were investigated in a mouse model of myocardial infarction. AAV9-RXFP1 vectors were generated and injected in adult male CD1 mice. Up-regulation of *Rxfp1* was confirmed via quantitative polymerase chain reaction, and overexpressing animals showed increased sensitivity to relaxin-induced ventricular inotropic response. Overexpressing animals also demonstrated reduced infarct size and preserved cardiac function 24 hours after ischemia-reperfusion. Up-regulation of RXFP1 via AAV9 vectors has potential therapeutic utility in preventing adverse remodeling after myocardial infarction. (J Am Coll Cardiol Basic Trans Science 2022;7:53–63)

Relaxin-2 is a peptide hormone recognized primarily for its physiological role in modulating maternal hemodynamic function during the latter stages of mammalian pregnancy (1,2). Placentally derived relaxin-2 facilitates fetal demands by increasing cardiac output, vascular compliance, and renal blood flow (1). However, further investigation of relaxin-2-mediated effects revealed the diverse functionality of the hormone in various organ systems, including the male reproductive system, skeletal and connective tissue, central nervous system, and cardiac tissue (1). In the heart, relaxin-2 elicits signaling in cardiomyocytes, resident fibroblasts, and endothelial cells and has been shown to confer protection in several models of myocardial damage and heart failure (2,3). Acute administration of relaxin-2 has been shown to improve survival; reduce infarct size, inflammation, and immune cell-mediated damage; and prevent fibrosis and arrhythmogenesis in animal models of myocardial infarction (MI) (2,4-6). Previous studies from our laboratory demonstrated that endothelial nitric oxide synthase (eNOS)-dependent signaling and reduction of NACHT, LRR, and PYD domains-containing protein 3 inflammasome activity mediate protection of the murine heart after acute ischemia-reperfusion (IR) injury (6). Long-term treatment with relaxin-2 prevents adverse remodeling and hinders progression toward heart failure in animal models of ischemic, isoproterenol-induced, and pressure-overload variants of heart failure (7-9). Nevertheless, the limitations associated with long-term relaxin-2 administration, including production costs (owing to incorporation of intrapeptide disulfide linkages) (2), short in vivo half-life (3-4 hours), and the need for routine, parenteral administration, challenge the translational impact of direct use of the hormone (10).

The G-protein coupled receptor relaxin family peptide receoptor 1 (RXFP1) serves as the cognate receptor for relaxin-2 in tissues. RXFP1 possesses unique leucine-rich repeats in the N terminus of the receptor, and these residues enable ligand binding and activation (3). The regulation of RXFP1 expression in the failing heart is not fully understood and could directly influence the efficacy of relaxin-2 treatment. For instance, beta-adrenergic activity (as observed in heart failure due to neurohormonal dysregulation) can reduce RXFP1 expression in cardiomyocytes (11). Finally, a potential mismatch in receptor-hormone-associated expression changes could also account for the observed increase in relaxin-2 expression in the failing heart.

In our present study, we investigated the consequences of acute myocardial IR injury and subsequent cardiac adverse remodeling in mice overexpressing RXFP1. Overexpression of RXFP1 was achieved through adeno-associated virus serotype 9 (AAV9) vectors capable of cardiotropic gene therapy. Overexpressing RXFP1 can potentially overcome the limitations posed by ligand-based options, as AAV9 vectors have been shown to ensure stable overexpression for extended periods of time following initial delivery (12).

METHODS

A detailed description of experimental groups and animals, preparation of AAV9 plasmids and vectors, Millar catheterization, the MI protocol for IR injury, echocardiography, infarct size and scar size estimation, isolation of primary cardiomyocytes, and the simulated ischemia and reoxygenation (SIRO) protocol is included in the Supplemental Appendix.

STUDY DESIGN AND ANIMALS. Sample sizes were rationally chosen given our prior experience with IR

in animal models and expected rates of intra- or postoperative mortality. Adult CD1 mice (8 weeks old) were purchased from Charles River Laboratories. All animal procedures, including tail vein injections for viral vector delivery, IR surgery, echocardiography, Millar catheterization, and sample acquisition, were performed in strict adherence to guidelines for the care and use of laboratory animals, as updated by the National Institutes of Health (8th edition, 2011). The aforementioned techniques are approved for our implementation by the Virginia Commonwealth University Institutional Animal Care and Use Committee. Mice were injected with 100 μL of saline, empty vector (VEC), or AAV9-RXFP1 via the tail vein and were allowed to incubate for 4 weeks prior to further experimentation. For the IR surgery, mice were anesthetized with intraperitoneal pentobarbital (70 mg/kg) and subsequently intubated. Thoracotomy was performed, and the left anterior descending coronary artery was identified and ligated around a polyethylene tube for 30 minutes to induce cardiac ischemia, followed by reperfusion.

STATISTICAL ANALYSIS. Data from the experiments were assessed for normality using the Shapiro-Wilk normality test. For normal distributions, data are reported as mean ± SEM. For comparison between 2 groups, an unpaired Student's *t*-test was used. For 3 or more groups, 1-way (or 2-way) analysis of variance was used to determine statistical significance, followed by Tukey's post hoc method for multiple pairwise comparisons. For skewed distributions, data are summarized as median (IQR). To compare 2 datasets, the Wilcoxon rank sum test was used to determine significance. For all comparisons, P values <0.05 were considered to indicate statistical significance. Statistical analyses were performed using GraphPad version 8 (GraphPad Software).

RESULTS

INJECTION OF AAV9 PARTICLES UP-REGULATES CARDIAC EXPRESSION OF RXFP1. The AAV9 vector was chosen for cardiac delivery of RXFP1 transgenes to facilitate overexpression. To ensure global cardiac up-regulation of RXFP1, a cytomegalovirus (CMV) promoter was inserted upstream of RXFP1 complementary deoxyribonucleic acid, measuring 2.2 kb, in the AAV9 vector (**Figure 1A**). As detailed in the Supplemental Methods, viral particles were generated using a helper-free plasmid and a human embryonic kidney 293 cell transfection system in the vector core at the University of Pennsylvania. To determine the optimal titer for in vivo experimentation, 3 different doses of viral vectors were given intravenously to adult male CD1 mice 6 to 8 weeks of age and allowed to incubate for 4 weeks. After this period, cardiac tissue was isolated for gene expression using real-time polymerase chain reaction. *Rxfp1* expression was up-regulated at all 3 doses (**Figure 1B**). Therefore, a viral dose of 1×10^{11} genomes was used for subsequent experimentation. Overexpression of *Rxfp1* in AAV9-administered mice was confirmed through messenger ribonucleic acid (mRNA) in cardiac tissue lysates, as well as in primary cardiomyocyte isolates (**Figures 1C and 1D**). Downstream signaling of RXFP1 is facilitated by various modulators, including members of the mitogen-activated protein kinase (MAPK) family (p44/p42 MAPK), and is transduced by various second messengers. Phosphorylation of p44/p42 MAPK, a downstream event of RXFP1 activation, was also significantly higher in mice overexpressing *Rxfp1* 4 weeks after AAV9-RXFP1 administration (**Figure 1E**).

OVEREXPRESSION OF RXFP1 IN THE LEFT VENTRICLE INCREASES SERELAXIN-INDUCED INOTROPIC RESPONSE. Left ventricular (LV) pressure-volume (PV) analysis was performed using Millar catheterization of mice. To test whether high concentrations of serelaxin influenced cardiac cycle physiology, healthy CD1 male controls were used. A bolus dose of 1 mg/kg serelaxin was delivered subcutaneously, and PV loops were monitored for 15 minutes. Mice injected with serelaxin attained higher peak systolic pressures (ΔP_{max}) and $\Delta dP/dt_{max}$ and higher end-systolic pressure toward the end of cardiac ejection (**Figure 2A,** Supplemental Table 1). The upward-left shift of end-systolic pressure, along with increases in stroke volume and pressures, indicates an increase in contractility (inotropy). These effects were independent of preload (ventricular filling), as the slope for end-systolic PV relationship obtained after briefly turning off mechanical ventilation (eliciting a Valsalva-like reflex and increasing preload) was higher after injecting serelaxin (1 mg/kg) (**Figure 2B**). Therefore, the increase in pressures associated with relaxin administration is likely due to increased contractility and not due to changes in preload and afterload. End-diastolic pressure did not change among the groups. However, $\Delta dP/dT_{min}$, which is associated with isovolumetric relaxation, was lowered (increased in magnitude) upon administration of relaxin (Supplemental Table 1). The LV relaxation constant τ, which is independent of loading conditions, was also lower with treatment (Supplemental Table 1). Taken together, these findings suggest that relaxin possibly contributes to both increased contractility during systole and active relaxation during diastole. Alternatively, no significant changes

FIGURE 1 Feasibility Data for Using AAV-RXFP1 Vectors for Cardiotropic Expression

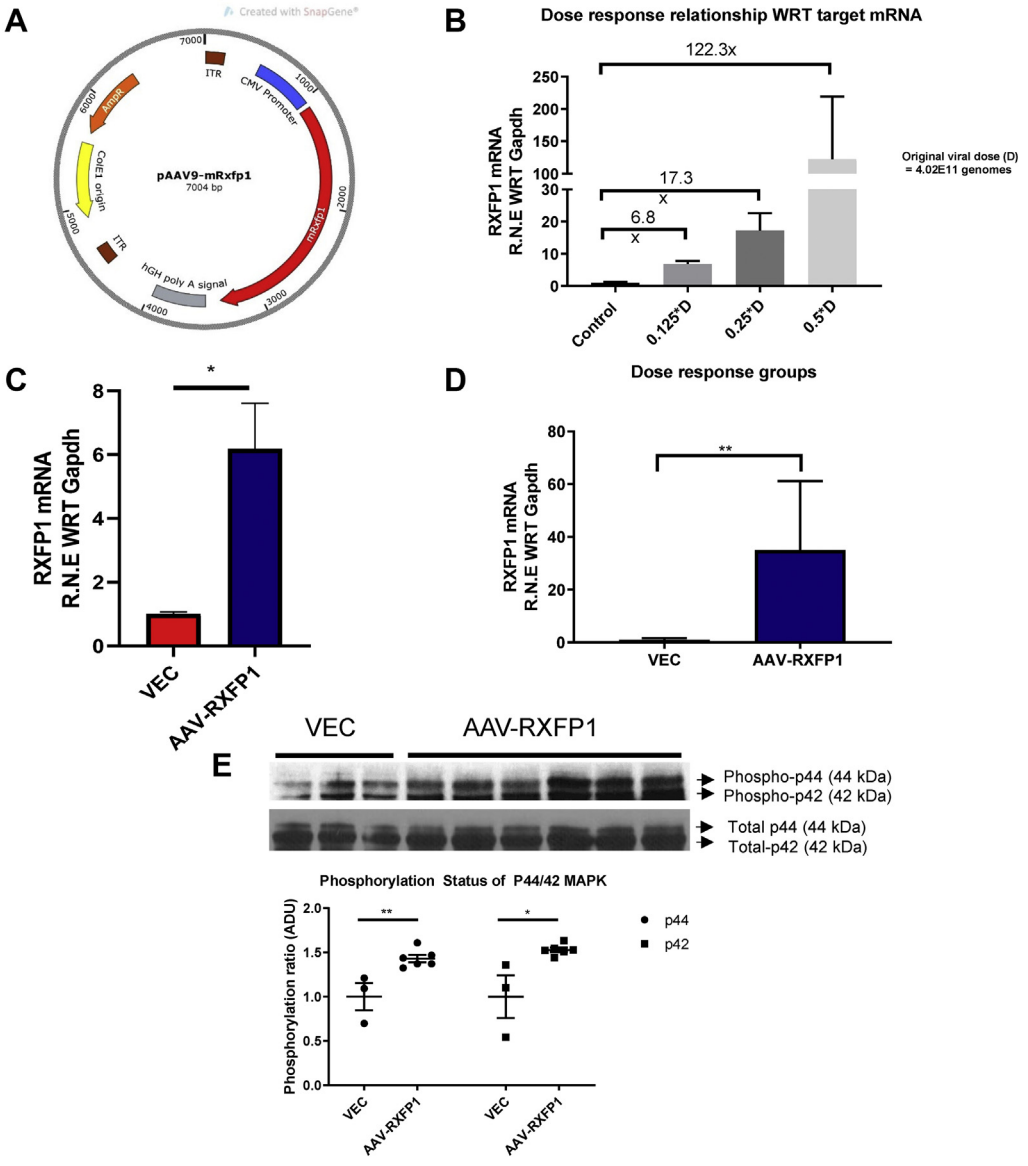

(A) Schematic outlining the plasmid design with the transgene incorporated downstream of the cytomegalovirus (CMV) promoter. **(B)** Dose-response relationship measuring the messenger ribonucleic acid (mRNA) levels of relaxin family peptide receptor 1 (RXFP1) 4 weeks after injection of adeno-associated virus (AAV)-RXFP1; quantitative polymerase chain reaction analysis shows increased expression of *Rxfp1* mRNA at all doses. For subsequent experimentation, 1×10^{11} viral genomes per mouse was chosen. **(C)** Significantly higher mRNA expression of *Rxfp1* in cardiac tissue lysates when treated with AAV-RXFP1 compared with empty vector (VEC) (1×10^{11} genomes/mouse, n = 4 for all experimental groups). **(D)** Significantly higher expression of *Rxfp1* mRNA was observed in cardiomyocytes isolated from AAV-RXFP1 mice when primary cells were isolated 4 weeks after injection with AAV-RXFP1 (n = 5 for all experimental groups). **(E)** Increased phosphorylation of p44/p42 mitogen-activated protein kinase (MAPK) in cardiac tissue lysates extracted from AAV-RXFP1 mice (n = 6) compared with VEC mice (n = 3). For **C**, 1-way analysis of variance with Tukey post hoc analysis was used. For **D**, the Mann-Whitney *U* test was performed to compare the skewed distributions. For **E**, unpaired Student's *t*-test was used for comparisons between the groups. *$P < 0.05$. **$P < 0.01$. ADU = arbitrary densitometric units.

FIGURE 2 **Representative PV Loop Tracings Before and After Intervention in Control Mice**

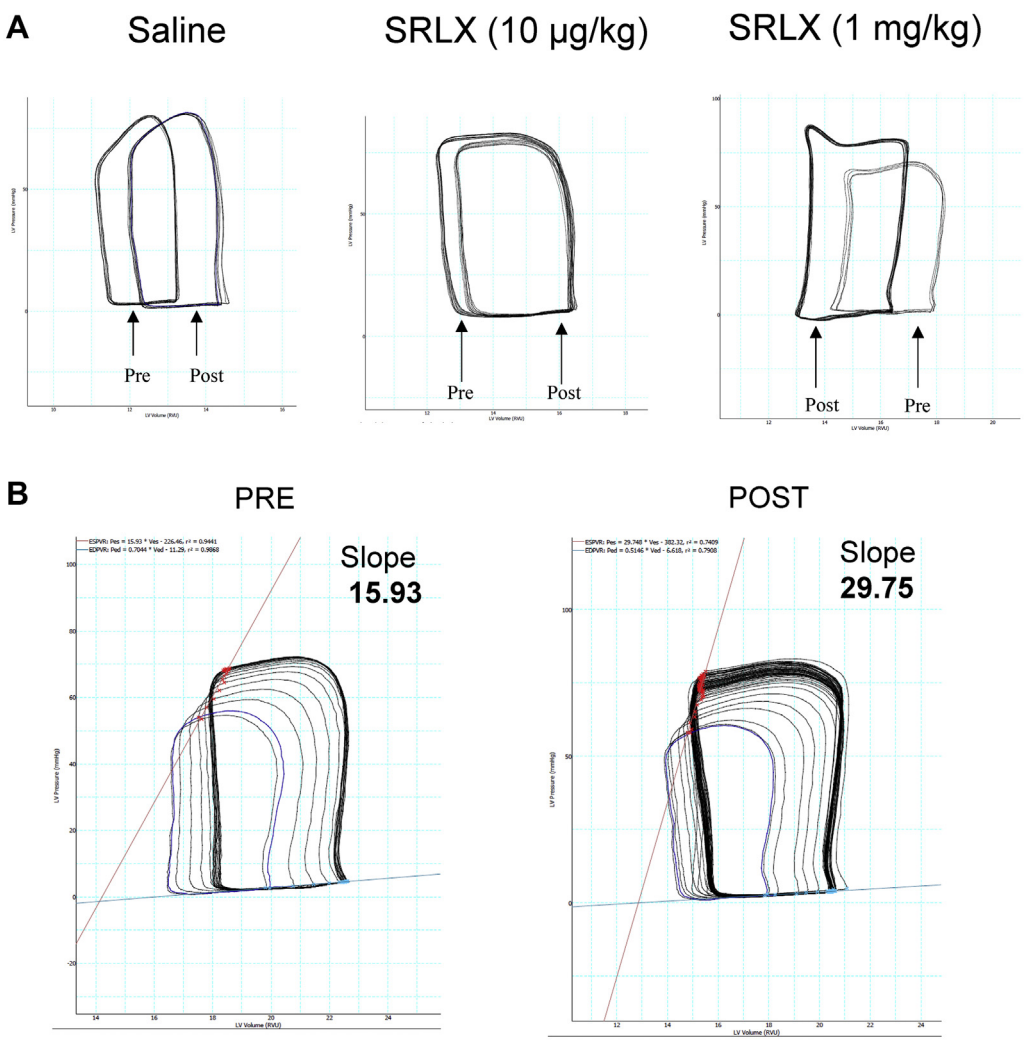

(A) Representative pressure-volume (PV) loops showing cardiac function showing baseline function (pre) and function after injection (within 15 minutes; post) of either saline or serelaxin (SRLX) (10 μg/kg and 1 mg/kg) acute doses delivered intraperitoneally. End-systolic pressure and peak systolic pressure (P_{max}) are visibly elevated in animals injected with 1 mg/kg serelaxin (Supplemental Table 1). **(B)** Representative tracings of acute changes in PV loops upon stoppage of mechanical ventilation (leading to increased left ventricular [LV] filling). The slope of the end-systolic PV relationship (ESPVR) was lower when preload increase was facilitated prior to the injection of 1 mg/kg serelaxin (pre). After the intervention, and upon confirming the stabilization of any drug-induced effects on the PV loops, mechanical ventilation was turned off to obtain the ESPVR slope (post). The higher slope after intervention suggests that the observed increases in contractile pressures are preload independent. EDPVR = end-diastolic pressure-volume relationship; Ped = end-diastolic pressure; Pes = end-systolic pressure; RVU = relative volume unit; Ved = end-diastolic volume; Ves = end-systolic volume.

in the aforementioned parameters were observed when animals were treated with a lower dose of serelaxin (10 μg/kg) (**Figure 2A,** Supplemental Table 1).

To test whether manipulating RXFP1 expression levels influenced the sensitivity of the PV relationships to exogenously administered relaxin, mice from the viral vector groups were treated with a 10 μg/kg dose of serelaxin. Mice injected with AAV-RXFP1 (as opposed to the VEC group) showed increased sensitivity to the lower dose, as observed through changes in ΔP_{max}, $\Delta dP/dt_{max}$, end-systolic pressure, $\Delta dP/dT_{min}$, and τ, recapitulating the trends observed when CD1 male controls were injected with high-dose (1 mg/kg) serelaxin (**Figures 3A to 3G**). An increased trend (without statistical significance) was also detected in the change in stroke volume and stroke work (Supplemental Figures S1A and S1B), and no significant differences were noted in the change in heart rate. Baseline

FIGURE 3 Millar Tracings in Transfected Mice After Administration of Low-Dose Serelaxin

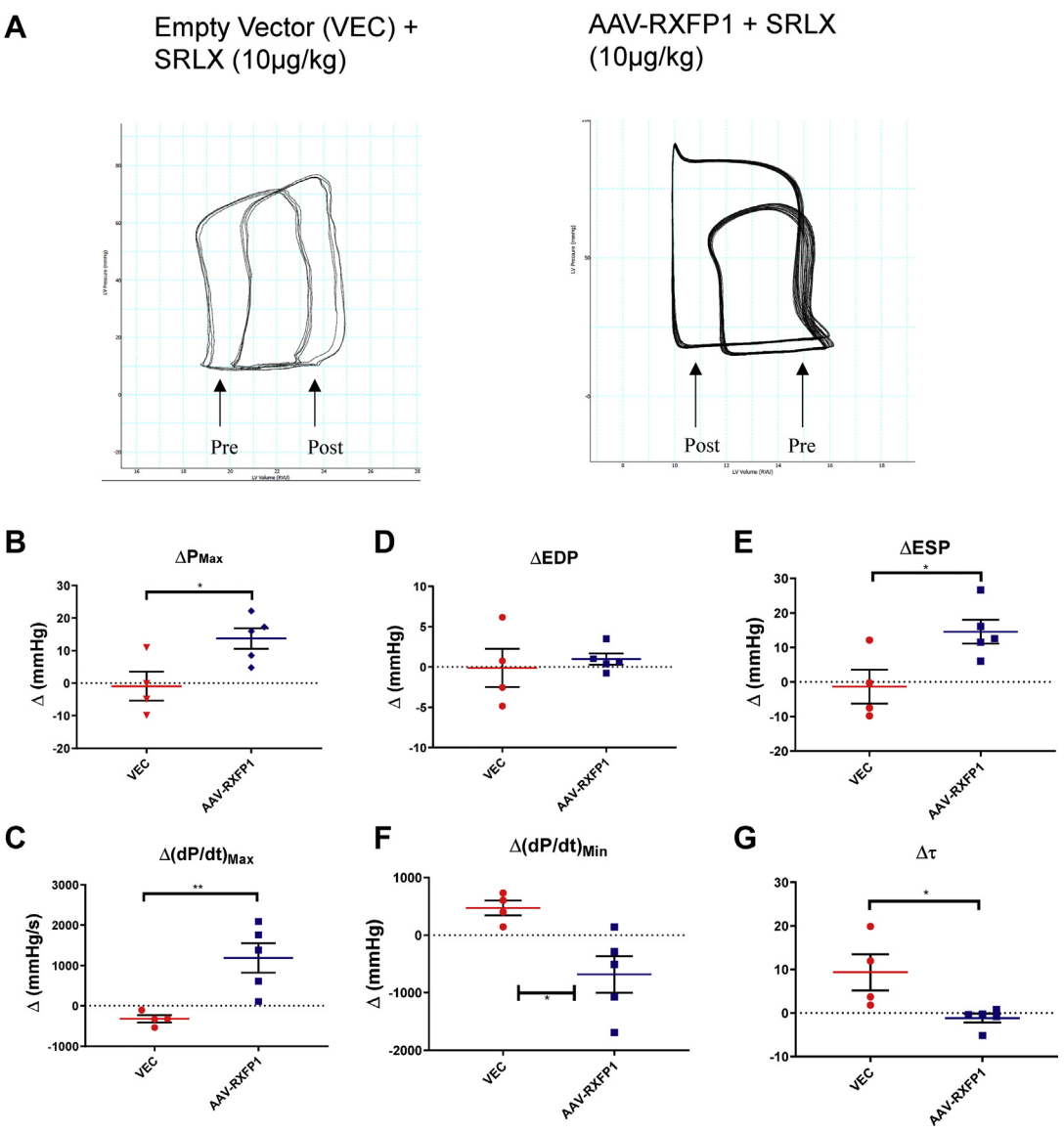

(A) Representative PV loops tracings in VEC and AAV-RXFP1 mice before (pre) and after (post) administration of low-dose serelaxin (10 μg/kg) intraperitoneally. PV-associated parameters are subsequently quantified. **(B)** The change in peak systolic pressure (P_{Max}) was significantly higher in the AAV-RXFP1 group (13.75 ± 3.13 mm Hg/s vs −0.94 ± 4.46 mm Hg/s in VEC group). **(C)** The change in $(dP/dt)_{Max}$ was also significantly higher with serelaxin treatment in AAV-RXFP1 group (1,191 ± 365.5 mm Hg/s vs −319.8 ± 125.3 mm Hg/s in VEC group). **(D)** No net changes in end-diastolic pressure (EDP) were detected between the groups (0.97 ± 0.70 mm Hg/s in AAV-RXFP1 group vs −0.11 ± 2.39 mm Hg/s in VEC group; P = NS). **(E)** The increase in end-systolic pressure (ESP) was significantly higher in the AAV-RXFP1 group with serelaxin (14.58 ± 3.428 mm Hg/s vs −1.33 ± 4.92 mm Hg/s in VEC group). **(F)** Increased magnitude of change in $(dP/dt)_{Min}$ was observed in AAV-RXFP1 animals when treated with serelaxin (−682 ± 318.8 mm Hg/s vs 384 ± 133.3 mm Hg/s in VEC group). **(G)** The load-independent relaxation constant τ is lowered after treatment with relaxin in the AAV-RXFP1 group (net change −1.15 ± 1.03 in AAV-RXFP1 group and 5.83 ± 3.109 in VEC group). For **B to G**, n = 4 for VEC and n = 5 for AAV-RXFP1; unpaired student's *t*-test was used to compare datasets. *P < 0.05. **P < 0.01. Abbreviations as in Figures 1 and 2.

FIGURE 4 **Infarct Size and Functional Parameters Post-MI in Transfected Mice**

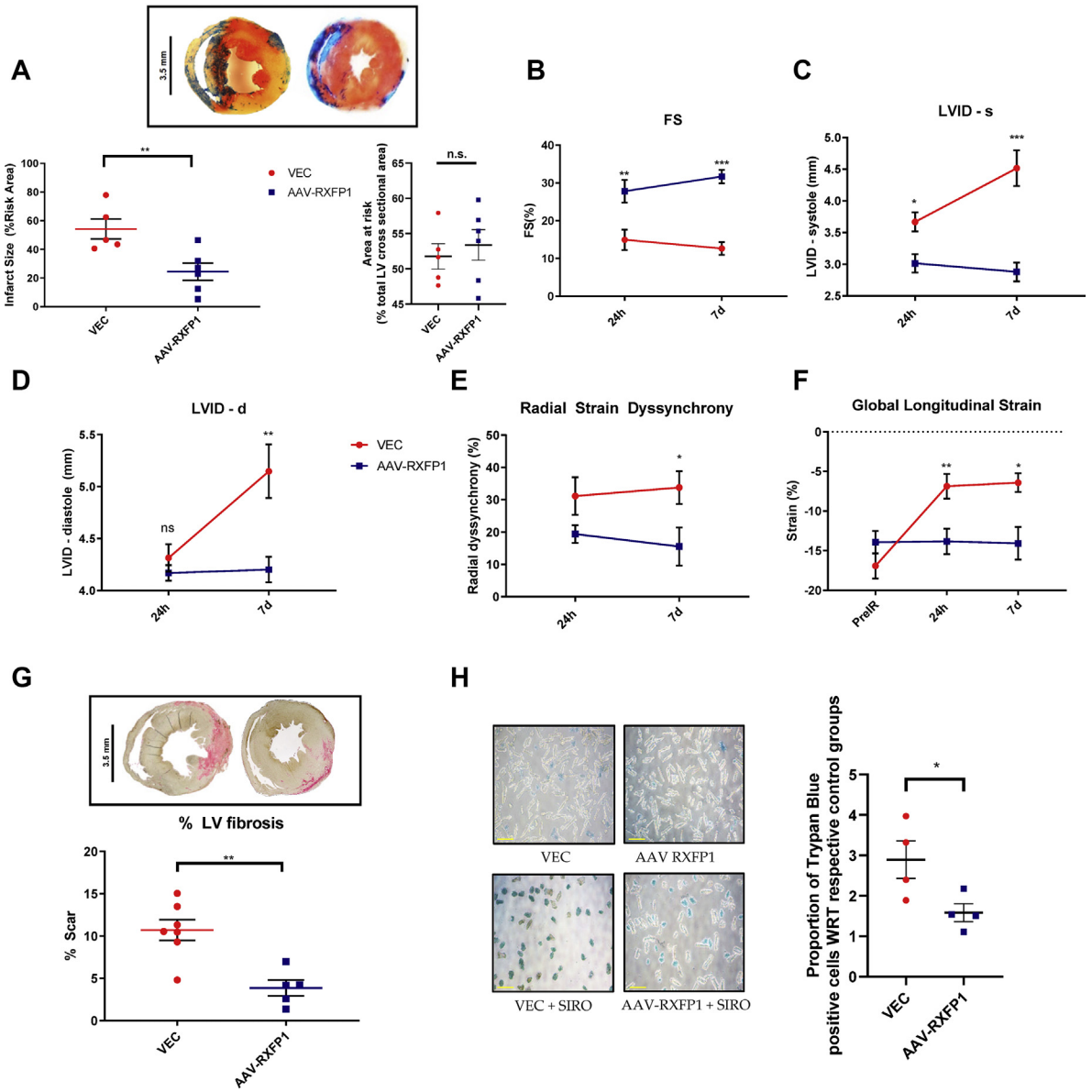

(A) Infarct size was significantly lower in AAV-RXFP1 mice (24.42% ± 5.95%) compared with VEC mice (54.22% ± 15.70%) when expressed as a percentage of area at risk. **Bar** represents 3.5 mm. Area at risk did not differ between the 2 groups (53.40% ± 2.16% in AAV-RXFP1 vs 51.77% ± 1.80% in VEC). **(B)** Fractional shortening (FS) was significantly higher in the AAV-RXFP1 group at 24 hours (27.81% ± 2.993% vs 14.94% ± 2.68% in VEC) and 7 days (31.68% ± 1.77% vs 12.64% ± 1.69% in VEC). **(C)** Left ventricular internal diameter at systole (LVID - s) was significantly smaller in AAV-RXFP1 mice at 24 hours (3.01 ± 0.14 mm vs 3.67 ± 0.15 mm in VEC) and 7 days (2.87 ± 0.15 mm vs 4.51 ± 0.28 mm in VEC). **(D)** Left ventricular internal diameter at diastole (LVID - d) was not significantly different at 24 hours between the groups but was significantly smaller in AAV-RXFP1 mice at 7 days (4.20 ± 0.12 mm vs 5.15 ± 0.26 mm in VEC). **(E)** Radial dyssynchrony among the left ventricular (LV) long-axis segments was not significantly different between the AAV-RXFP1 and VEC groups at 24 hours (19.39% ± 2.73% vs 31.14% ± 5.84%, respectively) but was significantly higher in the VEC group at 7 days (15.53% ± 5.87% vs 33.79% ± 5.039%). **(F)** Global longitudinal strain was significantly higher in magnitude in AAV-RXFP1 mice at 24 h (−13.84% ± 1.61% vs −6.86% ± 1.56% in VEC) and 7 days (−14.08% ± 2.07% vs −6.42% ± 1.17% in VEC). **(G)** LV scar size was significantly smaller at 7 days post-myocardial infarction (MI) in AAV-RXFP1 mice (3.86% ± 0.94%) than in VEC mice (10.71% ± 1.23%), expressed as a percentage of LV tissue (**bar** represents 3.5 mm). **(H)** The proportion of trypan blue-positive cells (compared with baseline in the corresponding non-simulated ischemia and reoxygenation [SIRO] controls) was significantly lower in myocytes isolated from AAV-RXFP1 animals compared with VEC (1.58 ± 0.22 vs 2.89 ± 0.46, respectively). For **A and H**, unpaired Student's *t*-test was used (n = 5 for VEC and AAV-RXFP1). For **B to F** (n = 5-10), 2-way analysis of variance with post hoc Bonferroni test was used. For **G**, unpaired Student's *t*-test was used to compare scar sizes between VEC (n = 7 for VEC, n = 5 for AAV-RXFP1). **Bar** represents 100 μm. *$P < 0.05$. **$P < 0.01$. ***$P < 0.001$. PreIR = pre-ischemia/reperfusion; other abbreviations as in Figures 1 and 2.

parameters (prior to injection of serelaxin) did not vary among the wild-type CD1, VEC, and AAV-RXFP1 groups (Supplemental Table 2). The association between ventricular contractility/relaxation and acute relaxin treatment has not been physiologically characterized in vivo before, and up-regulation of RXFP1 led to a more pronounced response to relaxin exposure in our experiments.

RXFP1 OVEREXPRESSION PROTECTS MICE FROM MYOCARDIAL IR INJURY. After the 4-week incubation period for the AAV9-injected mice, cardiac function was assessed via echocardiography to detect any changes in healthy, overexpressing mice. Animals from all the experimental groups had no significant differences in LV fractional shortening and heart rate (Supplemental Table 3). Mice were subjected to IR injury via left anterior descending coronary artery ligation for 30 minutes to induce myocardial ischemia. After 24 hours of reperfusion, infarct size was measured using 2,3,5-triphenyltetrazolium chloride staining. AAV-RXFP1 mice had a significantly lower infarct size, expressed as a percentage of at-risk area (**Figure 4A**). The area at risk did not differ between the groups. Functional parameters were recorded at 24 hours and 7 days post-MI. Short-axis M-mode views demonstrated preserved fractional shortening in AAV-RXFP1 mice compared with VEC mice (**Figure 4B**). LV internal diameter at systole was smaller in the AAV-RXFP1 group, indicating more robust contractile function compared with the VEC group (**Figure 4C**). Although the internal diastolic diameter did not significantly differ between the groups at the 24-hour time point, the trend diverged to significance at 7 days as the remodeling process ensued (**Figure 4D**). Subsequently, long-axis views were obtained for speckle-tracking and strain analysis. Preservation of systolic function was evident in the AAV-RXFP1 group upon assessment of radial dyssynchrony (**Figure 4E**). Most important, global longitudinal strain (GLS) was significantly higher in magnitude in the treated group at the 24-hour and 7-day time points (**Figure 4G**). The extent of adverse remodeling post-MI was higher in the VEC group, as LV sections from AAV-RXFP1 mice had a significantly smaller percentage of LV fibrosis (**Figure 4H**).

Adult primary cardiomyocytes isolated from VEC and AAV RXFP1 mice were subjected to hypoxia in an ischemia buffer, followed by SIRO with myocyte media. A subset of cells from the experimental groups were not subjected to the SIRO conditions and were used as controls for the experiment. The percentage of cell death was estimated by the number of trypan blue-positive cells, and a baseline was obtained for the non-SIRO controls. The percentage of dead cells in the SIRO groups was expressed as a proportion of this baseline from the corresponding non-SIRO groups. Primary myocytes from RXFP1-overexpressing mice had a smaller proportion of dead cells after SIRO (**Figure 4I**).

DISCUSSION

The cardioprotective benefits of relaxin therapy have been demonstrated in numerous preclinical studies. Although the protective mechanisms significantly influence fibroblast signaling (13), immune cell infiltration (14), sterile inflammation (6,15), and prevention of microvascular damage and leakage (16), relaxin treatment also influences calcium dynamics (5), electric properties (via associated increases in sodium channel [17] and connexin expression [18]), and energetics (AMPK-Akt pathway [19]) by directly acting on cardiomyocytes. In our previous work, we demonstrated the cardioprotective effects of serelaxin in mitigating cardiac IR injury by inhibiting the activation of the NACHT, LRR, and PYD domains-containing protein 3 inflammasome in an eNOS-dependent manner (6). More recently, we showed that B7-33, a functionally selective RXFP1 agonist, reduces tunicamycin-induced endoplasmic reticular stress in primary cardiomyocytes via activation of p44/p42 MAPK (20), an event central to several of the protective mechanisms elicited by relaxin signaling, including eNOS activation, inhibition of transforming growth factor β signaling, and reactive oxygen species production (2,21). In the present study, phosphorylation of p44/p42 MAPK was up-regulated in cardiac tissue lysates after overexpression of RXFP1, suggesting a mechanistic link explaining the observed outcomes.

Several constraints limit the direct therapeutic usage of relaxin to address ischemic heart disease, including a short half-life, need for parenteral administration, and production costs, as mentioned earlier. Because of the paucity of high-fidelity antibodies capable of accurately detecting G-protein coupled receptor expression in biological tissues, characterizing the expression of RXFP1 in the normal and diseased ventricular myocardium is challenging. Taking these factors into consideration, we sought to investigate alternative approaches with increased potential for translational impact for relaxin therapy in ischemic heart disease. By using AAV9 vectors to induce RXFP1 up-regulation in the heart, we attempted to: 1) understand the functional role of RXFP1 overexpression in the myocardium; 2) elicit exogenous agonist-independent myocardial protection, attributable to either constitutive activity of RXFP1 or compensatory increases in myocardial

relaxin over the course of disease evolution; and 3) ascertain the potential of AAV9 gene therapy as a vector for RXFP1-induced cardioprotection. To take advantage of the pleiotropic benefits associated with RXFP1 signaling in cardiac fibroblasts and endothelial cells (in addition to cardiomyocytes), a CMV promoter was inserted upstream of the *Rxfp1* transgene. Injection of AAV-RXFP1 vectors led to a significant up-regulation of *Rxfp1* mRNA 4 weeks postincubation, indicating a robust transcription of viral complementary deoxyribonucleic acid in myocardial tissue, as well as isolated primary cardiomyocytes. Given the lack of consistency in detecting RXFP1 protein in a reproducible and replicable manner using commercially available antibodies, RXFP1 up-regulation was not confirmed via western blot. However, the observed phosphorylation of p44/p42 MAPK, along with changes in cardiac physiology upon treatment with low-dose serelaxin in AAV-RXFP1 group, are consistent with the up-regulation of *Rxfp1* mRNA.

The canonical signaling pathways associated with RXFP1 involve a Gα subunit-induced, biphasic activation of adenylyl cyclase isotypes, leading to cyclic adenosine monophosphate production shortly following ligand activation. The G$\beta\gamma$ subunit dissociates from the heterotrimeric G protein complex upon activation to activate p44/p42 MAPK signaling, which has been implicated in several cardioprotective pathways (3,22). However, RXFP1 forms a signalosome complex in the absence of nanomolar-range relaxin concentration and demonstrates constitutive activity that is sensitive to even attomolar (10-18 M) ranges of relaxin expression (23). Although the therapeutic relevance of this pathway is yet uncertain, it is possible that protection of myocardial function in AAV-RXFP1 mice occurs through these mechanisms.

In the present study, despite the changes associated with overexpression-induced downstream signaling, physiological parameters at baseline, including fractional shortening and heart rate, did not vary among the experimental groups. Previously, intraperitoneal administration of 10 μg/kg serelaxin in our mice led to plasma concentrations close to 1 ng/mL within minutes following injection (6). To test whether higher concentrations of relaxin led to changes in cardiac function, LV pressures and volumes were measured using Millar catheterization before and after the administration of low (10 μg/kg) and high (1 mg/kg) doses of serelaxin in healthy CD1 male controls. High-dose serelaxin led to a previously unreported in vivo finding involving acute increases in contractility, as evidenced by increases in peak systolic pressure, dP/dt_{max}, and end-systolic pressure and the characteristic shape of the PV loop. These effects were preload independent, as the end-systolic PV relationship slope also increased with high-dose serelaxin treatment. Relaxin-induced ventricular inotropy has been sparsely reported, because of species-dependent differences in receptor expression and variations in methodology (24,25) (ex vivo, myofilament force development, etc). Interestingly, relaxin-induced increases in contractility were attributed to increased phosphorylation of myosin-binding protein C, troponins T and I, and increased Ca^{2+} sensitivity, without increasing myofilament adenosine triphosphate consumption (24). This differs mechanistically from catecholamine-induced inotropy, in which energy consumption is increased because of protein kinase A activation (26). Treatment with relaxin also improved relaxation kinetics (preload and afterload independent) in the myocardium, suggesting improved calcium dynamics during the active relaxation. These findings have significant therapeutic implications, as relaxin-induced inotropy and lusitropy (relaxation) can potentially increase stroke volume and meet the circulatory demands in ischemic heart disease, without increasing energetic demands due to high stroke work. AAV-RXFP1 mice showed inotropic effects even at a lower dose of relaxin, suggesting increased sensitivity to the hormone upon receptor up-regulation.

Adeno-associated viral vectors are a preferred vector for delivery of transgenes to the myocardium because of low immunogenicity and a predictable course of transfection (27). The lack of *rep* and *cap* genes prevents self-assembly, secondary infection, and integration into the host genome. The viral genome remains as episomal inclusions within the nucleus, reducing the likelihood of random insertions within the host genome and inducing mutagenesis (27). The unique 3-dimensional structure conferred by the variable surface regions of the AAV9 capsid (as opposed to other serotypes) enables cardiac tropism (variable surface region IX) (28). The differential expression of viral transgenes was strongly dependent on the route of administration; intravenous delivery strongly favors uptake of AAV9 particles by cardiac and hepatic tissue (29). Interestingly, it was shown that intravascular delivery of 1×10^{11} genomes led to a strong fluorescent signal in histologic sections of heart and liver when AAV9-CMV-green fluorescent protein particles were delivered (29). Expression in spleen, lung, kidney, brain, and muscle was minimal. The use of a CMV promoter led to sustained green fluorescent protein expression only in the heart, while liver green fluorescent protein levels declined 8 weeks postinjection (29). In our study, 1×10^{11} AAV-RXFP1 viral genomes led to a strong up-regulation of

Rxfp1. Although achieving cardiac-specific overexpression was not the goal of the present study, targeted expression could possibly be attained by using a targeted promoter such as cardiac troponin T (30) (chicken cardiac troponin). Further experimentation is necessary to address concerns related to off-target expression.

Up-regulation of RXFP1 in the ventricular tissue led to a significant decline in infarct size 24 hours post-MI (24.42% vs 54.22% in the AAV-RXFP1 and VEC groups, respectively). This reduction is comparable with that demonstrated in our previous work, in which acute cardioprotection was achieved with serelaxin (10 μg/kg) (6). The functional effects of cardioprotection were also observed in short-axis parameters including fractional shortening and LV internal diameter at systole. GLS, which is a stronger predictor of mortality than LV ejection fraction in patients with acute heart failure (31), was also significantly attenuated in the VEC but not the AAV-RXFP1 group at 24 hours. Interestingly, trends in fractional shortening, LV internal diameter (at systole and diastole), and GLS diverged further at the 7-day time point. These findings suggest continued protection from overexpression in addition to the infarct-sparing effects of RXFP1 up-regulation. Future studies will be directed toward understanding the effect of adverse remodeling by up-regulating RXFP1 as a rescue strategy and delivering the viral vectors after MI. Scar size at 7 days was significantly smaller in the treatment group, implicating the antifibrotic effects of RXFP1 signaling. Although several mechanisms have been implicated, Wnt signaling-induced blockade of the transforming growth factor-β pathway was demonstrated in fibroblasts exposed to relaxin (32). Recently, it was shown that RXFP1 heterodimerizes with angiotensin II receptor to transduce signaling in fibroblasts. The significance of this signaling paradigm is yet to be determined in our model of RXFP1 overexpression (33). Finally, in vitro experimentation in our study showed that myocytes from RXFP1-overexpressing mice had a reduced number of trypan blue-positive cells upon SIRO, indicating reduced cell death in this context.

Our present experimental design was focused on examining the feasibility of using AAV9 vectors to overexpress RXFP1 in the ventricular myocardium. AAVs were previously used to up-regulate sarcoplasmic/endoplasmic reticulum Ca^{2+}-ATPase in the CUPID (A Study of Genetically Targeted Enzyme Replacement Therapy for Advanced Heart Failure) trial to address clinical endpoints of heart failure (34). Although the trial failed to successfully improve the clinical course in patients, the finding that <1% of cardiomyocytes were successfully infected by the AAVs (because of high dose requirements) could have potentially affected the outcomes of the trial (35). In the context of adverse remodeling, targeting cardiomyocytes specifically downstream of an infarct could be more effective and translationally achievable. Nevertheless, transitioning to human trials would require adequate assessment of safety profiles and dosing strategies.

FUNDING SUPPORT AND AUTHOR DISCLOSURES

This study was supported by the American Heart Association (grant 18PRE33990001 to Mr Devarakonda), the Wright Center for Clinical and Translational Research Center (Wright Scholarship to Mr Devarakonda), and the National Institutes of Health (grants R01HL142281, R21AG053654, R01HL133167, and R35HL155651 to Dr Salloum). The authors have reported that they have no relationships relevant to the contents of this paper to disclose.

ADDRESS FOR CORRESPONDENCE: Dr Fadi N. Salloum, Division of Cardiology, Box 980204, Virginia Commonwealth University, 1101 East Marshall Street, Room 7-070, Richmond, Virginia 23298, USA. E-mail: fadi.salloum@vcuhealth.org.

PERSPECTIVES

COMPETENCY IN MEDICAL KNOWLEDGE: Our research is centered on the topics of MI and resultant adverse remodeling and congestive heart failure. By targeting relaxin signaling via the overexpression of RXFP1 receptors, we show a potential therapeutic strategy to confer cardioprotection post-MI. Given its clinical relevance, this work directly relates to the medical knowledge component of the 6 domains promulgated by the Accreditation Council on Graduate Medical Education as part of competency-based learning in cardiovascular medicine.

TRANSLATIONAL OUTLOOK: Relaxin is a pleiotropic hormone shown to confer cardioprotective properties in several animal models of heart disease. In the context of MI, the protective signaling associated with relaxin therapy has been shown to reduce inflammation, fibrosis, and arrhythmogenesis. We designed and produced AAV9 vectors capable of up-regulating RXFP1, the relaxin receptor, in the heart and demonstrated the preservation of cardiac tissue and function post-MI in overexpressing mice. Gene therapy via RXFP1 up-regulation could play a novel role in protecting ischemic myocardium and preventing adverse remodeling, mitigating the clinical burden of heart failure.

REFERENCES

1. Bathgate RAD, Halls ML, van der Westhuizen ET, Callander GE, Kocan M, Summers RJ. Relaxin family peptides and their receptors. *Physiol Rev*. 2013;93(1):405–480.

2. Devarakonda T, Salloum FN. Heart disease and relaxin: new actions for an old hormone. *Trends Endocrinol Metab*. 2018;29(5):338–348.

3. Halls ML, Bathgate RAD, Sutton SW, Dschietzig TB, Summers RJ. International Union of Basic and Clinical Pharmacology. XCV. Recent advances in the understanding of the pharmacology and biological roles of relaxin family peptide receptors 1-4, the receptors for relaxin family peptides. *Pharmacol Rev*. 2015;67(2):389–440.

4. Bani D, Masini E, Bello MG, Bigazzi M, Sacchi TB. Relaxin protects against myocardial injury caused by ischemia and reperfusion in rat heart. *Am J Pathol*. 1998;152(5):1367–1376.

5. Masini E, Bani D, Bello MG, Bigazzi M, Mannaioni PF, Sacchi TB. Relaxin counteracts myocardial damage induced by ischemia-reperfusion in isolated guinea pig hearts: evidence for an involvement of nitric oxide. *Endocrinology*. 1997;138(11):4713–4720.

6. Raleigh JV, Mauro AG, Devarakonda T, et al. Reperfusion therapy with recombinant human relaxin-2 (serelaxin) attenuates myocardial infarct size and NLRP3 inflammasome following ischemia/reperfusion injury via eNOS-dependent mechanism. *Cardiovasc Res*. 2017;113(6):609–619.

7. Zhang J, Qi YF, Geng B, et al. Effect of relaxin on myocardial ischemia injury induced by isoproterenol. *Peptides*. 2005;26(9):1632–1639.

8. Shuai XX, Meng Y, Lu YX, et al. Relaxin-2 improves diastolic function of pressure-overloaded rats via phospholamban by activating Akt. *Int J Cardiol*. 2016;218:305–311.

9. Samuel CS, Cendrawan S, Gao X-M, et al. Relaxin remodels fibrotic healing following myocardial infarction. *Lab Investig*. 2011;91(5):675–690.

10. Agoulnik AI, Agoulnik IU, Hu X, Marugan J. Synthetic non-peptide low molecular weight agonists of the relaxin receptor 1. *Br J Pharmacol*. 2017;174(10):977–989.

11. Moore X-L, Su Y, Fan Y, et al. Diverse regulation of cardiac expression of relaxin receptor by α1- and β1-adrenoceptors. *Cardiovasc Drugs Ther*. 2014;28:221–228.

12. Bish LT, Morine K, Sleeper MM, et al. Adeno-associated virus (AAV) serotype 9 provides global cardiac gene transfer superior to AAV1, AAV6, AAV7, and AAV8 in the mouse and rat. *Hum Gene Ther*. 2008;19(12):1359–1368.

13. Sassoli C, Chellini F, Pini A, et al. Relaxin prevents cardiac fibroblast-myofibroblast transition via Notch-1-mediated inhibition of TGF-β/Smad3 signaling. *PLoS ONE*. 2013;8(5):e63896.

14. Nistri S, Chiappini L, Sassoli C, Bani D. Relaxin inhibits lipopolysaccharide-induced adhesion of neutrophils to coronary endothelial cells by a nitric oxide-mediated mechanism. *FASEB J*. 2003;17(14):2109–2111.

15. Pinar AA, Yuferov A, Gaspari TA, Samuel CS. Relaxin can mediate its anti-fibrotic effects by targeting the myofibroblast NLRP3 inflammasome at the level of caspase-1. *Front Pharmacol*. 2020;11:1201.

16. Gao XM, Su Y, Moore S, et al. Relaxin mitigates microvascular damage and inflammation following cardiac ischemia–reperfusion. *Basic Res Cardiol*. 2019;114(4):30.

17. Henry BL, Gabris B, Li Q, et al. Relaxin suppresses atrial fibrillation in aged rats by reversing fibrosis and upregulating Na^+ channels. *Heart Rhythm*. 2016;13(4):983–991.

18. Wang D, Zhu H, Yang Q, Sun Y. Effects of relaxin on cardiac fibrosis, apoptosis, and tachyarrhythmia in rats with myocardial infarction. *Biomed Pharmacother*. 2016;84:348–355.

19. Aragón-Herrera A, Feijóo-Bandín S, Rodríguez-Penas D, et al. Relaxin activates AMPK-AKT signaling and increases glucose uptake by cultured cardiomyocytes. *Endocrine*. 2018;60(1):103–111.

20. Devarakonda T, Mauro AG, Guzman G, et al. B7-33, a functionally selective relaxin receptor 1 agonist, attenuates myocardial infarction-related adverse cardiac remodeling in mice. *J Am Heart Assoc*. 2020;9(8):e015748.

21. Sarwar M, Du X, Dschietzig TB, Summers RJ. The actions of relaxin on the human cardiovascular system. *Br J Pharmacol*. 2017;174:933–949.

22. Chow BSM, Chew EGY, Zhao C, Bathgate RAD, Hewitson TD, Samuel CS. Relaxin signals through a RXFP1-pERK-nNOS-NO-cGMP-dependent pathway to up-regulate matrix metalloproteinases: the additional involvement of iNOS. *PLoS ONE*. 2012;7(8):e42714.

23. Halls ML, Cooper DMF. Sub-picomolar relaxin signalling by a pre-assembled RXFP1, AKAP79, AC2, β2-arrestin 2, PDE4D3 complex. *EMBO J*. 2010;29(16):2772–2787.

24. Shaw EE, Wood P, Kulpa J, Feng HY, Summerlee AJ, Pyle WG. Relaxin alters cardiac myofilament function through a PKC-dependent pathway. *Am J Physiol Heart Circ Physiol*. 2009;297(1):29–36.

25. Dschietzig T, Alexiou K, Kinkel HT, Baumann G, Matschke K, Stangl K. The positive inotropic effect of relaxin-2 in human atrial myocardium is preserved in end-stage heart failure: role of Gi-phosphoinositide-3 kinase signaling. *J Card Fail*. 2011;17(2):158–166.

26. Ali DC, Naveed M, Gordon A, et al. β-Adrenergic receptor, an essential target in cardiovascular diseases. *Heart Fail Rev*. 2020;25(2):343–354.

27. Colella P, Ronzitti G, Mingozzi F. Emerging issues in AAV-mediated in vivo gene therapy. *Mol Ther Methods Clin Dev*. 2018;8:87–104.

28. DiMattia MA, Nam H-J, Van Vliet K, et al. Structural insight into the unique properties of adeno-associated virus serotype 9. *J Virol*. 2012;86(12):6947–6958.

29. Chen BD, He CH, Chen XC, et al. Targeting transgene to the heart and liver with AAV9 by different promoters. *Clin Exp Pharmacol Physiol*. 2015;42(10):1108–1117.

30. Prasad K-M, Xu Y, Yang Z, Acton S, French B. Robust cardiomyocyte-specific gene expression following systemic injection of AAV: in vivo gene delivery follows a Poisson distribution. *Gene Ther*. 2011;18(1):43–52.

31. Park JJ, Park JB, Park JH, Cho GY. Global longitudinal strain to predict mortality in patients with acute heart failure. *J Am Coll Cardiol*. 2018;71(18):1947–1957.

32. Martin B, Gabris B, Barakat AF, et al. Relaxin reverses maladaptive remodeling of the aged heart through Wnt-signaling. *Sci Rep*. 2019;9(1):18545.

33. Chow BSM, Kocan M, Shen M, et al. AT1R-AT2R-RXFP1 functional crosstalk in myofibroblasts: impact on the therapeutic targeting of renal and cardiac fibrosis. *J Am Soc Nephrol*. 2019;30(11):2191–2207.

34. Greenberg B, Butler J, Felker GM, et al. Calcium upregulation by percutaneous administration of gene therapy in patients with cardiac disease (CUPID 2): a randomised, multinational, double-blind, placebo-controlled, phase 2b trial. *Lancet*. 2016;387(10024):1178–1186.

35. Hulot JS, Ishikawa K, Hajjar RJ. Gene therapy for the treatment of heart failure: promise postponed. *Eur Heart J*. 2016;37(21):1651–1658.

KEY WORDS gene therapy, ischemia-reperfusion injury, LV function, relaxin, RXFP1

APPENDIX For a supplemental Methods section, tables, and a figure, please see the online version of this paper.